Check for updates

Chemistry–A European Journal
Research Article
doi.org/10.1002/chem.202302850
Chemistry Europe
European Chemical Societies Publishing
www.chemeurj.org

n-Type Fullerene-Carbon Dots: Synthesis and Electrochemical and Photophysical Properties

Andrés Ferrer-Ruiz,[a] Juan Manuel Moreno-Naranjo,[a, b] Laura Rodríguez-Pérez,[a] Sergio Ramírez-Barroso,[a] Nazario Martín,*[a, c] and María Ángeles Herranz*[a]

Dedicated to Prof. Maurizio Prato on the occasion of his 70th birthday

The covalent incorporation of C_{60} and C_{70} derivatives of the well-known n-type organic semiconductor PCBM ([6,6]-phenyl-C61-butyric acid methyl ester) onto carbon dots (CD) is described. Morphological and structural characterization reveal combined features of both pristine starting materials (CD and PCBM). Electrochemical investigations evidenced the existence of additional reduction processes to that of CD or PCBM precursors, showing rich electron-acceptor capabilities, with multistep processes in an affordable and narrow electrochemical window (*ca.* 1.5 V). Electronic communication in the obtained nanoconjugated species were derived from steady-state absorption and emission spectroscopies, which showed bathochromically shifted absorptions and emissions well entering the red region. Finally, the lower fluorescence quantum yield of CD-PCBM nanoconjugates, compared with CD, and the fast decay of the observed emission of CD, support the existence of an electronic communication between both CD and PCBM units in the excited state.

Introduction

Carbon-based nanomaterials present outstanding electronic, optical and mechanical properties, which make them candidates for a wide variety of applications.[1] Within this large family, where fullerenes,[2] carbon nanotubes,[3] or graphene[4] are outstanding representative members, carbon dots (CD)[5] have recently received the attention of the research community considering their stability, facile fabrication, low toxicity, good solubility, and remarkable photo-physical properties.[6] In particular, the photoluminescence that these materials exhibit is quite promising for the fields of biosensing, biomedicine and in optoelectronic devices.[7]

CD are nanosized materials (<10 nm) that can be easily obtained at low-cost by bottom-up methodologies. Small organic molecules, oligomers or polymers, rich in amino, hydroxyl and carboxylic groups, allowed the preparation of these nanomaterials by means of dehydration, condensation, crosslinking and carbonization.[8] The precursors chosen and the reaction conditions of the synthesis -combustion, pyrolysis, ultrasound assisted, solvothermal or hydrothermal, and microwave-assisted methods- have a great impact on the final structure (surface groups) and properties of CD (chirality, optoelectronics).[9]

By means of heteroatom doping, the optoelectronic properties of CD are modulated.[10] Nitrogen doping raises the electron density, resulting in a lowering of the HOMO levels and in wider bandgaps. In general, nitrogen has demonstrated to elevate the charge transfer efficiency in CD.[11] On the contrary, boron as a dopant causes a decrease in charge density and is used, in general, as an electron-deficient dopant in CD.[12] Other examples with fluorine, selenium, silicon, or sulfur doping of CD have also been reported.[7a,13] Remarkably, the highest electronegativity of fluorine and its strong electron withdrawing tendency decreases the energy gap, presenting the obtained CD red-shifted excitation and emission wavelengths with regard to undoped CD.[14]

Besides heteroatom doping, a strategy to create versatile and functional systems based on CD is to rely on the post-synthetic covalent functionalization of CD. In such a way, the electron accepting or electron donating properties of CD can be complemented with the electronic nature of the interfaced species.[15] CD have been covalently grafted with electron-donating porphyrins,[16] phthalocyanines,[17] and π-extended

[a] Dr. A. Ferrer-Ruiz, J. M. Moreno-Naranjo, Dr. L. Rodríguez-Pérez, Dr. S. Ramírez-Barroso, Prof. Dr. N. Martín, Prof. Dr. M. Á. Herranz
Department of Organic Chemistry, Faculty of Chemistry
Universidad Complutense de Madrid
28040 Madrid (Spain)
E-mail: nazmar@ucm.es
maherran@ucm.es
Homepage: http://www.nazariomartingroup.com
[b] J. M. Moreno-Naranjo
(current address)
Department of Chemistry and Molecular Sciences Research Hub
Imperial College London
White City Campus, London (UK)
[c] Prof. Dr. N. Martín
IMDEA-Nanociencia
c/Faraday 9, Campus Cantoblanco, 28049 Madrid (Spain)

Supporting information for this article is available on the WWW under https://doi.org/10.1002/chem.202302850

© 2023 The Authors. Chemistry - A European Journal published by Wiley-VCH GmbH. This is an open access article under the terms of the Creative Commons Attribution Non-Commercial NoDerivs License, which permits use and distribution in any medium, provided the original work is properly cited, the use is non-commercial and no modifications or adaptations are made.

© 2023 The Authors. Chemistry - A European Journal published by Wiley-VCH GmbH

tetrathiafulvalenes,[18] performing as charge-transfer electron-acceptors or as energy-transfer materials, as described for porphyrin-functionalized CD. Naphthalene monoimides[19] and 11,11,12,12-tetracyano-9,10-anthra-*p*-quinodimethane (TCAQ)[20] units were also covalently linked to CD and resulted in the formation of charge-separated states where, upon photo-induced electron-transfer, the electron-donating properties of CD were evidenced.

In light of these synthetic approaches leading to adjustable functionalization and opto-electronic properties, CD have been recently employed as a replacement of the sensitizer in dye sensitized solar cells (DSSCs)[21] or as additives in perovskite solar cells (PSCs).[22] Moreover, the chance to employ CD as charge transport materials in solar cells was evaluated by mixing N-doped CD functionalized with different thiophene-containing groups and the fullerene derivative [6,6]-phenyl-C61-butyric acid methyl ester ($PC_{61}BM$), in solution and in solid blends.[23] In thin films of CD:$PC_{61}BM$ blends, the complete quenching of the CD fluorescence is observed. Furthermore, the presence of long lived $PCBM^{\bullet-}$ species were detected, as a result of photoinduced electron-transfer reaction from the thiophene-modified N-CD. The photoresponse of supramolecularly assembled thin films, formed by negatively charged water soluble carbon dots and positively charged fulleropyrrolidine adducts (FP) and porphyrins (P), also confirmed the interest of CD in light harvesting and solar energy conversion systems. An enhancement of about a 300% of the short circuit current density in P-FP/CD thin films, when compared with a more traditional P-FP solar device, was observed.[24]

Motivated by these results, the covalent combination of CD and fullerenes was explored in this work. Specifically, for the anchoring to CD, a derivative of the widely employed in organic photovoltaics $PC_{61}BM$[25] and the analog with the C_{70} molecule, $PC_{71}BM$,[26] were used. The aim of the formation of CD-$PC_{61}BM$ and CD-$PC_{71}BM$ nanoconjugates was to improve the solubility and processability of PCBMs in non-polar solvents and to obtain new nanomaterials with enhanced electron-transport properties.

The combined opto-electronic properties of CD and PCBM, as well as the good grafting ability that these materials might exhibit, could be essential for targeted applications, especially in the fields of photovoltaics, but also photocatalysis and sensing.

Results and Discussion

Here, we build on a multi-component approach, under controlled pressure, using citric acid and urea as starting materials to produce CD.[27] The precursors were heated in a microwave reactor maintaining the pressure constant at 15 bar for 5 min., the controlled pressure limits the escape of gaseous byproducts from the solution and allows CD nucleation and carbonization to terminate at an early stage.[28] The obtained CD are characterized by an amorphous carbogenic core and a surface rich in carboxylic acid groups.[18,20]

The synthesis of $PC_{61}BM$ and $PC_{71}BM$ was carried out following the synthetic protocols previously reported.[25,26] The methyl esters of both derivatives were reduced with diisobutylaluminium hydride (DIBAL) to generate the final alcohols **$PC_{61}BM$-OH** and **$PC_{71}BM$-OH**.[29] For simplicity, only the major isomer (α-isomer, *ca.* 85% yield) of the four possible siteisomers[30] (α, β, γ, and δ) obtained for **$PC_{71}BM$-OH** is shown (Scheme 1). The work continued with the mixture obtained, without further purification of the different siteisomers.

The attachment of **$PC_{61}BM$-OH** and **$PC_{71}BM$-OH** to CD was carried out using the same strategy followed in previous work of the group.[18,20] Briefly, the as-prepared CD were treated with thionyl chloride under heating conditions to transform the carboxylic acids to acid chlorides. These material reacted *in situ*

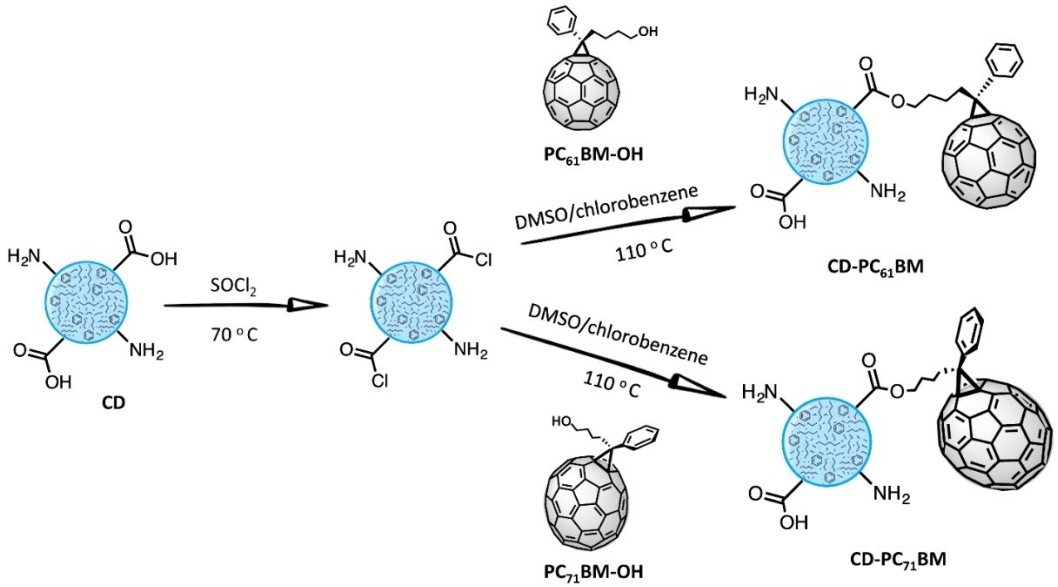

Scheme 1. Illustrative scheme of the synthesis of **CD-$PC_{61}BM$** and **CD-$PC_{71}BM$**.

© 2023 The Authors. Chemistry - A European Journal published by Wiley-VCH GmbH

15213765, 0, Downloaded from https://chemistry-europe.onlinelibrary.wiley.com/doi/10.1002/chem.202302850 by Universidad Autonoma De Madrid, Wiley Online Library on [08/01/2024]. See the Terms and Conditions (https://onlinelibrary.wiley.com/terms-and-conditions) on Wiley Online Library for rules of use; OA articles are governed by the applicable Creative Commons License

with **$PC_{61}BM$-OH** or **$PC_{71}BM$-OH** dissolved in a mixture of DMSO/chlorobenzene 1/1 to yield **CD-$PC_{61}BM$** and **CD-$PC_{71}BM$** nanoconjugates (Scheme 1). After isolation and purification (see Experimental Section for details), the morphology of both **CD-$PC_{61}BM$** and **CD-$PC_{71}BM$** nanoconjugates was investigated by means of AFM. The measurements demonstrated the presence of quite homogeneous objects with an average height of 3.2 ± 1.0 nm for **CD-$PC_{61}BM$** (Figure S1) and 3.3 ± 0.8 nm for **CD-$PC_{71}BM$** (Figure 1). As expected, the obtained hybrids after the anchoring of C_{60} or C_{70} units to CD, have similar dimensions and are larger than those of the starting batch of CD, with an average height of 1.9 ± 0.6 nm (Figure S1) or the isolated fullerenes in CD and **$PC_{61}BM$-OH** or **$PC_{71}BM$-OH** mixtures (*ca.* 1.1 ± 0.2 nm, Figure S2).

To confirm that the observed objects in the AFM are due to the PCBM units attached to the CD and not to non-covalently bonded aggregates, TGA analyses were performed with the starting CD, the molecular fullerenes, a physical mixture of both of them (1 : 1 in weighted amounts) and, the formed covalent hybrids (Figures 1 and S3). In Figure 1b, it is noticed the CD accused weight loss around 200 °C, and the more constant weight loss after this temperature is observed. On the other hand, **$PC_{61}BM$-OH** suffers a major loss at approximately 380 °C and a second loss at 550 °C. Both samples follow a similar molecular decomposition pattern, since their weight losses occur in a narrow temperature range forming well-defined derivative peaks. Conversely, **CD-$PC_{61}BM$** decomposes in a soft and consistent way throughout the whole temperature range, with a pattern more similar to those observed in materials. In addition, it is important to highlight that the decomposition pattern of **CD-$PC_{61}BM$** does not have any abrupt weight loss, which could match with the main decomposition temperature of **$PC_{61}BM$-OH**. Similar results were obtained for **CD-$PC_{71}BM$** (Figure S3), which exhibits a constant weight loss with the lack of any abrupt loss, which can match with the features discerned in **$PC_{71}BM$-OH**. For the physical mixtures of CD and **$PC_{61}BM$-OH** or **$PC_{71}BM$-OH**, a weight loss around 200 °C (most probably resulting from the loss of carboxylic groups in the form of CO_2) is particularly evident. Small maxima in the derived curves between 380 °C and 500 °C, coinciding with the main losses observed in **$PC_{61}BM$-OH** and **$PC_{71}BM$-OH**, were also perceived Therefore, TGA analyses confirm the lack of free PCBM-OH molecules in the functionalized CD hybrids. This information supports the covalent coupling, thus ruling out the possibility that fullerenes be interacting by non-covalent forces with CD.

The CD-fullerene hybrids were subsequently investigated by FTIR. C_{60} derivatives present a characteristic vibrational mode at 527 cm^{-1},[31] which is perfectly distinguished in both, the **$PC_{61}BM$-OH** and **CD-$PC_{61}BM$** spectra (Figure S4) and is indicative of the successful synthesis of **CD-$PC_{61}BM$**. Furthermore, in the starting CD spectrum, no signal is observed in this region, which indicates that the signal in **CD-$PC_{61}BM$** is stemming from the $PC_{60}BM$ anchored to CD.

Considering the C_{70} derivatives, it is important to note that C_{70} itself presents more signals in its FTIR spectrum due to the loss of symmetry, in comparison with the icosahedral C_{60} molecule. Indeed, C_{70} exhibits five remarkable vibrational modes located at 533, 579, 645, 674 and 700 cm^{-1}.[31] These signals are perfectly recognized in the **$PC_{71}BM$-OH** and **CD-$PC_{71}BM$** spectra as shown in Figure 2. Moreover, these signals do not appear in the spectrum of the starting CD, indicating that they come from the $PC_{70}BM$ in the functionalized CD. In addition, the changes observed in the band at 1800–1600 cm^{-1} after the functionalization process could be indicative of the formation of new ester groups.

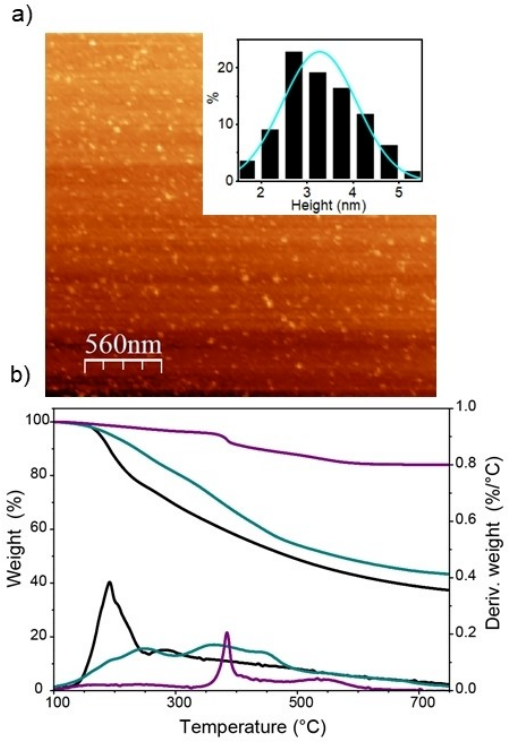

Figure 1. a) Representative AFM image of **CD-$PC_{71}BM$**. Inset: Height histogram with a curve fit of the data using a Gaussian model (statistical analysis carried out with one hundred elements of the sample). Average height: 3.3 ± 0.8 nm. b) TGA and first derivative under inert conditions of CD (black), **$PC_{61}BM$-OH** (purple) and **CD-$PC_{61}BM$** (cyan).

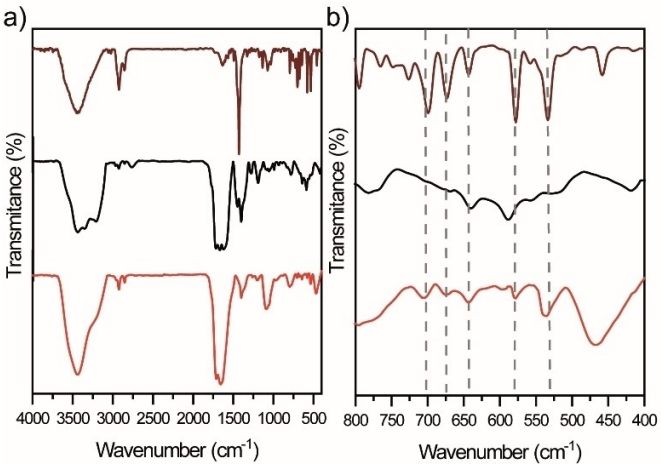

Figure 2. a) FTIR spectra of **$PC_{71}BM$-OH** (dark red), CD (black) and **CD-$PC_{71}BM$** (red). b) Expansion in the range of 800–400 cm^{-1} of the spectra showed in a).

© 2023 The Authors. Chemistry - A European Journal published by Wiley-VCH GmbH

15213765, 0, Downloaded from https://chemistry-europe.onlinelibrary.wiley.com/doi/10.1002/chem.202302850 by Universidad Autonoma De Madrid, Wiley Online Library on [08/01/2024]. See the Terms and Conditions (https://onlinelibrary.wiley.com/terms-and-conditions) on Wiley Online Library for rules of use; OA articles are governed by the applicable Creative Commons License

Both **CD-PC$_{61}$BM** and **CD-PC$_{71}$BM** were analyzed by XPS. The contributions stemming from the core levels of C 1s, O 1s, and N 1s were distinguished (Figure S5). The high-resolution C 1s core-level spectra of both hybrids (Figure 3) revealed the same species observed for CD originating from the core levels of C 1s (C–C/C=C), O 1s (C–O–C/C=O/O–C=O), and N 1s (C–O/C–N),[18,20] as well as the characteristic π- π* shake-up of fullerenes.[32] Herein, the shake-up of each compound is composed of two deconvolutions curves of low intensity, located at 288.4 and 289.6 eV for **CD-PC$_{61}$BM**, and 287.1 and 290.5 eV for **CD-PC$_{71}$BM**, which prompt to some graphitic character of the CD materials.[33] The XPS O 1s spectra can be curve-fitted into the two peak components attributable to the C–O and C=O species (Figure S5). Similarly to previous investigations, the N 1s lines showed the four components corresponding to graphitic-N, pyrrolic-N, –NH$_2$, and pyridinic-N (Figure S5).[18,20]

To evaluate the electronic properties of the novel nanoconjugates obtained, electrochemical measurements were carried out in a first instance. In cyclic voltammetry (CV) measurements, carried out in DMSO containing 0.1 M TBAPF$_6$ and under an argon atmosphere, CD show two evident irreversible oxidations corresponding to the amino groups and several irreversible reductions, the more prominent being observed at −2.03 and −2.31 V (Figure S6). After covalent modification with the **PC$_{61}$BM-OH** and **PC$_{71}$BM-OH** monoadducts, the electrochemical features of CD are not clearly discernible. A continuum of diffusion-controlled cathodic current, with an onset at around −0.5 V is observed. This behaviour could be attributed to the reductive charging of the **CD-PC$_{61}$BM** and **CD-PC$_{71}$BM** hybrids formed.

A closer inspection to the reductive electrochemistry of the CD nanoconjugates by differential pulse voltammetry (DPV) reveals the presence of several reduction processes of variable intensity ranging from *ca.* −0.54 to −2.32 V (Figure 4). Interestingly, besides the reductions corresponding to the C$_{60}$ or C$_{70}$ monoadducts (Figure S6),[34] which could be identified within the multistep reductive processes of CD nanoconjugates (see dashed lines in Figure 4), a more complex reductive picture evolves. A comparison with the voltammograms of physical mixtures of CD and **PC$_{61}$BM-OH** or **PC$_{71}$BM-OH** monoadducts, evidences the existence of additional reduction processes, which suggest the existence of electronic communication between the CD and the fullerenes. These multiple reductions, within a quite affordable electrochemical window, supports the interest of this type of materials as n-type semiconductors for electronic devices.

Next, we turned to evaluate the optical properties of the novel nanohybrids, which were initially characterized by UV-Vis-NIR spectroscopy. In Figure 5a, comparative spectra of CD, and the hybrid materials **CD-PC$_{61}$BM** and **CD-PC$_{71}$BM** are shown. In the synthesized hybrid materials, wider absorption ranges than that of the starting CD, fullerene materials, or mixtures of both are observed (Figure S7).

The UV-Vis-NIR spectrum of **PC$_{61}$BM-OH** exhibits two local maxima at 330 and 435 nm (Figure S7). The signal at 435 nm is considered a fingerprint of saturated C–C bonds between two hexagons of the C$_{60}$ sphere, regardless of the nature of the substituents involved.[35] For **CD-PC$_{61}$BM** shoulders for the main absorptions of **PC$_{61}$BM-OH** appear at *ca.* 342 and 450 nm, which seem to indicate that the fullerene absorptions are batochromically shifted in the hybrids. Similar results were found for **CD-PC$_{71}$BM**, where two small shoulders can be seen at *ca.* 373 and 440 nm, matching the absorption signals of **PC$_{71}$BM-OH** (Fig-

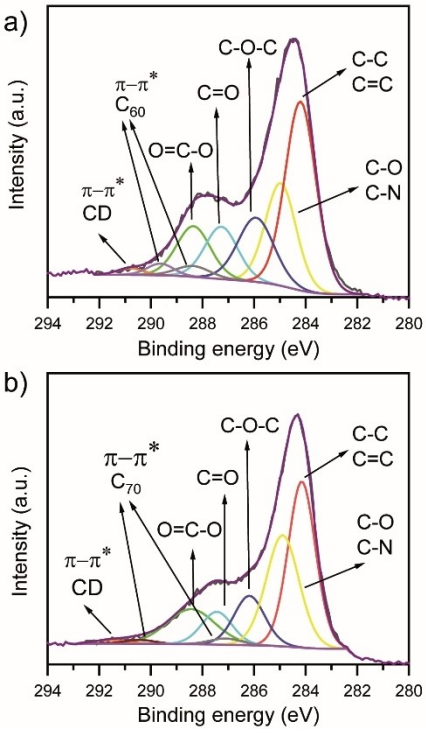

Figure 3. C 1s core-level component deconvolution spectra of: a) **CD-PC$_{61}$BM** and b) **CD-PC$_{71}$BM**.

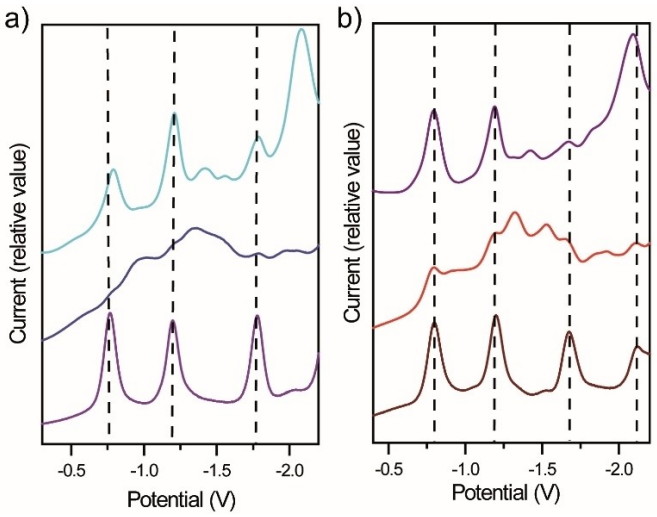

Figure 4. Differential pulse voltammograms of: a) From top to bottom: a CD and **PC$_{61}$BM-OH** mixture (cyan), **CD-PC$_{61}$BM** (blue) and **PC$_{61}$BM-OH** (purple); b) From top to bottom: a CD and **PC$_{71}$BM-OH** mixture (magenta), **CD-PC$_{71}$BM** (red) and **PC$_{71}$BM-OH** (maroon).

© 2023 The Authors. Chemistry - A European Journal published by Wiley-VCH GmbH

15213765, 0, Downloaded from https://chemistry-europe.onlinelibrary.wiley.com/doi/10.1002/chem.202302850 by Universidad Autonoma De Madrid, Wiley Online Library on [08/01/2024]. See the Terms and Conditions (https://onlinelibrary.wiley.com/terms-and-conditions) on Wiley Online Library for rules of use; OA articles are governed by the applicable Creative Commons License

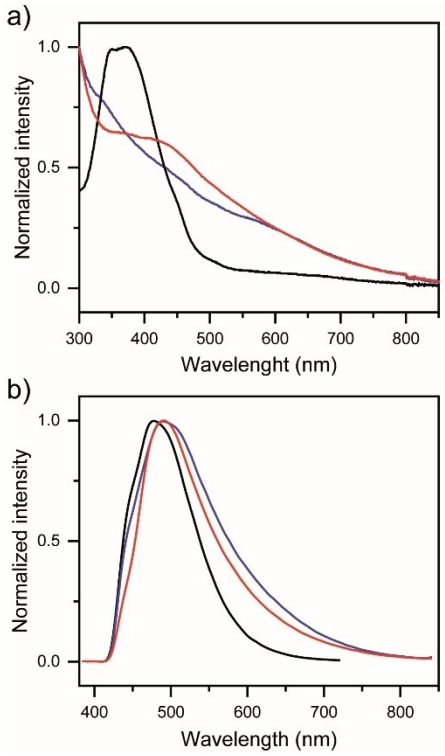

Figure 5. a) UV-Vis spectra of CD (black), **CD-PC$_{61}$BM** (blue) and **CD-PC$_{71}$BM** (red) in DMSO solutions. b) Emission spectra of CD (black), **CD-PC$_{61}$BM** (blue) and **CD-PC$_{71}$BM** (red) in DMSO solutions. The spectra were recorded with an excitation wavelength of 375 nm.

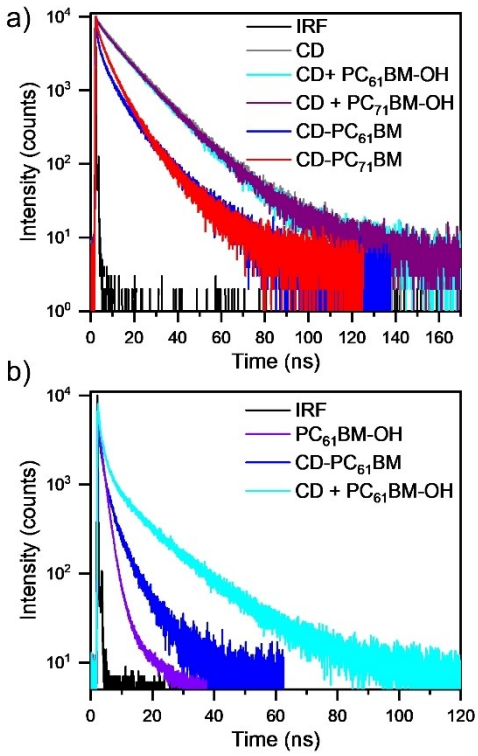

Figure 6. a) Time resolved fluorescence spectra, of the decay centered at 475 nm, for CD, a mixture of CD with **PC$_{61}$BM-OH** or **PC$_{71}$BM-OH**, **CD-PC$_{61}$BM** and **CD-PC$_{71}$BM** in DMSO solutions. b) Time resolved fluorescence spectra, of the decay centered between 700–720 nm, for **PC$_{61}$BM-OH**, **CD-PC$_{61}$BM** and, a mixture of CD with **PC$_{61}$BM-OH** in DMSO solutions. IRF refers to the Instrument Response Function.

ure S7). Again, quite shifted in comparison with its maxima visible at 374 and 460 nm. In principle, the obtained results might also go along with some sort of electronic communication between the CD and the fullerene derivatives in the ground state.

First proofs of excited-state interactions were deduced from fluorescence measurements. Herein, the emission maximum shifts from 475 nm in CD to 493 nm in **CD-PC$_{61}$BM** and **CD-PC$_{71}$BM**, with a tail emission that extends much further into the red reaching 800 nm (Figure 5b). Furthermore, the fluorescence quantum yield of CD decreased to 1.8 (**CD-PC$_{61}$BM**) and 2.3% (**CD-PC$_{71}$BM**) from a 17.2%. When CD are mixed with **PC$_{61}$BM-OH** or **CD-PC$_{71}$BM-OH** this value hardly ever changes (15.9 and 17.5%, respectively) and the emission spectra are very similar to that of CD (Figure S8b).

Time-resolved fluorescence allowed to monitor the decay of the CD maximum emission at 475 nm, which was fitted with a triexponential function,[36] with an intensity average lifetime of 14.0 ns and an amplitude average lifetime of 11.1 ns. This decay pattern is very similar for mixtures of CD with **PC$_{61}$BM-OH** and **PC$_{71}$BM-OH** and in great contrast with the fluorescence decay centred at 495 nm for the conjugated nanohybrids (Figure 6a). For **CD-PC$_{61}$BM** and **CD-PC$_{71}$BM** intensity average lifetimes of 8.2 and 7.4 ns were obtained, and amplitude average lifetimes of 2.8 and 4.3 ns, respectively. In this case, it is evident that there is a strong shortening of all the lifetimes due to the excited state of CD, which suggests a strong deactivation of CD by non-radiative pathways.

On the other hand, when analysed the fluorescence decay centered between 700–720 nm due to **PC$_{61}$BM-OH** and **PC$_{71}$BM-OH** emission (Figure S8a), the observed decays were fitted with a multiexponential function with intensity average lifetimes of 1.26 and 1.06 ns, and amplitude average lifetimes of 1.71 and 1.43 ns, respectively.[37] For the mixtures between fullerenes and CD, what is detected is a much longer decay (Figure 6b and Figure S9), which seems to correspond to the decay of the CD alone at this wavelength. In contrast, the fluorescence decay of **CD-PC$_{61}$BM** and **CD-PC$_{71}$BM** is slightly elongated (Figure 6b and Figure S9), which is also observed in the averaged times in intensity that become 3.2 and 3.3 ns for **CD-PC$_{61}$BM** and **CD-PC$_{71}$BM**, respectively. This effect could be due to the fact that the excited state of the fullerenes are activated, in addition to the irradiation, by an electronic transfer to the excited state of the CD.

Conclusions

In conclusion, we have successfully incorporated electron-acceptor fullerene derivatives (**PC$_{61}$BM-OH** and **PC$_{71}$BM-OH**) in the surface of CD by means of a covalent strategy that consisted in the previous activation of the carboxylic acids

© 2023 The Authors. Chemistry - A European Journal published by Wiley-VCH GmbH

15213765, 0, Downloaded from https://chemistry-europe.onlinelibrary.wiley.com/doi/10.1002/chem.202302850 by Universidad Autonoma De Madrid, Wiley Online Library on [08/01/2024]. See the Terms and Conditions (https://onlinelibrary.wiley.com/terms-and-conditions) on Wiley Online Library for rules of use; OA articles are governed by the applicable Creative Commons License

present in CD with $SOCl_2$ and the *in situ* incorporation of the electroactive molecules by esterification reactions. Evidences of the success of these reactions were obtained from AFM, TGA, FTIR, and XPS. Electrochemical measurements showed the existence of new reduction processes related with the covalent conjugation of the nanomaterials, which were complemented with the presence of batochromically shifted absorptions and emissions well entering the red region. In addition, the substantial decrease of the fluorescence quantum yields of CD compared with **CD-PC$_{61}$BM** and **CD-PC$_{71}$BM** species and, the different kinetics observed in the time-resolved fluorescence analysis of the main emissions, proved the electronic communication existing between CD and fullerenes in the excited state. The comparison with physical mixtures of CD and the fullerene precursor help distinguishing the covalent attached from the supramolecular interactions. Additional photophysical studies are been carried out in order to further evaluate the potential interest of CD-PCBM nanoconjugates as n-type semiconductor transport layers.

Experimental Section

Synthesis of CD. The CD were prepared under pressure considering the previously published protocol.[27] In a typical synthesis, citric acid (0.750 g) and urea (0.750 g) in 2.5 mL of deionized water were added into a microwave tube. This solution was heated in a microwave reactor for 5 min. maintaining the pressure at 15 bar. The resulting solution was poured into a 250 mL Erlenmeyer flask and was introduced in an oven at 100 °C one day in order to evaporate the water. The resulting black powder was washed with acetone with the aim of removing the polymeric residues formed during the synthesis. The solid was dried in an oven at 100 °C obtaining a shiny black powder (0.460 g). FTIR (KBr), ν (cm^{-1}): 1750–1500 (C=O stretching mode and C=C stretching mode). TGA (N_2 atmosphere): weight loss and temperature desorption (material stability): 58 %, 650 °C. XPS: % atomic: C (284.6 eV) = 59.5, O (531.6 eV) = 23.5, N (399.6 eV) = 17.0. UV-Vis (DMSO), λ_{max} (nm): 350, 375.

General procedure for the synthesis of CD-PC$_{61}$BM and CD-PC$_{71}$BM. CD (40 mg) were refluxed in $SOCl_2$ (10 mL) for 24 h. at 70 °C under argon atmosphere, the excess of $SOCl_2$ was then evaporated using argon as carrier gas. Over the modified CD were added **PC$_{61}$BM-OH** or **PC$_{71}$BM-OH** (20 mg) dissolved in 10 mL of a DMSO/chlorobenzene (1 : 1) mixture, and the reaction flask was sonicated for 2 h. under argon atmosphere for ensuring the complete dissolution of the reagents. Afterwards, the mixture was heated at 110 °C for 24 h. and under argon atmosphere. The resulting mixture was added over cold diethyl ether and was centrifuged at 6000 rpm for 10 min. Afterwards, the ether solution was removed, and fresh cold ether was added and the mixture centrifuged again in the same conditions. This process was repeated several times until the ether solution was colourless. The black solid was suspended in dichloromethane and separated by filtration through a 0.1 μm hydrophilic PTFE membrane and subjected to consecutive washings with toluene, MeOH and water until the collected solution was colourless. The obtained black powder were dried in vacuum to obtain a dark brown solid.

CD-PC$_{61}$BM. Obtained mass: 11.3 mg. FTIR (KBr), ν (cm^{-1}): 1750–1500 (C=O stretching mode) and 527 (C_{60} stretching mode). TGA (N_2 atmosphere): weight loss and temperature desorption (material stability): 54 %, 650 °C. XPS: % atomic: C (284.6 eV) = 63.3, O (531.6 eV) = 28.1, N (399.6 eV) = 8.6. UV-Vis (DMSO), λ_{max} (nm): 342, 450, 563.

CD-PC$_{71}$BM. Obtained mass: 16.6 mg. FTIR (KBr), ν (cm^{-1}): 1750–1500 (C=O stretching mode and C=C stretching mode) and 533, 579, 645, 674 and 700 (C_{70} stretching modes). TGA (N_2 atmosphere): weight loss and temperature desorption (material stability): 41 %, 650 °C. XPS: % atomic: C (284.6 eV) = 63.4, O (531.6 eV) = 27.9, N (399.6 eV) = 8.7. UV-Vis (DMSO), λ_{max} (nm): 373, 440.

Acknowledgements

Financial support by the Spanish Ministry of Science and Innovation (MICIN) through projects PID2020-115120GB–I00 and PID2020-114653RB–I00/AEI/10.13039/501100011033 and Comunidad de Madrid (CM) through project PR27/21-005 is acknowledged. The authors also thank CM and MICINN for the "(MAD2D-CM)-UCM" project, funded by the Recovery, Transformation and Resilience Plan, and the Next Generation European Union.

Conflict of Interests

The authors declare no conflict of interest.

Data Availability Statement

The data that support the findings of this study are available in the supplementary material of this article.

Keywords: carbon dots · fullerene · covalent synthesis · electron-transport · opto-electronics

[1] V. Georgakilas, J. A. Perman, J. Tucek, R. Zboril, *Chem. Rev.* **2015**, *115*, 4744–4822.
[2] a) H. W. Kroto, J. R. Heath, S. C. O'Brien, R. F. Curl, R. E. Smalley, *Nature* **1985**, *318*, 162–163; b) W. Krätschmer, L. D. Lamb, K. Fostiropoulos, D. R. Huffman, *Nature* **1990**, *347*, 354–358.
[3] a) S. Iijima *Nature* **1991**, *354*, 56–58; b) S. Iijima, T. Ichihashi, *Nature* **1993**, *363*, 603–605; c) D. S. Bethune, C. H. Kiang, M. S. de Vries, G. Gorman, R. Savoy, J. Vazquez, R. Beyers, *Nature* **1993**, *363*, 605–607.
[4] a) K. S. Novoselov, A. K. Geim, S. V. Morozov, D. Jiang, Y. Zhang, S. V. Dubonos, I. V. Grigorieva, A. A. Firsov, *Science* **2004**, *306*, 666–669; b) A. K. Geim, K. S. Novoselov, *Nat. Mater.* **2007**, *6*, 183–191.
[5] X. Xu, R. Ray, Y. Gu, H. J. Ploehn, L. Gearheart, K. Raker, W. A. Scrivens, *J. Am. Chem. Soc.* **2004**, *126*, 12736–12737.
[6] B. Yao, H. Huang, Y. Liu, Z. Kang, *Trends Chem.* **2019**, *1*, 235–246.
[7] a) Y. Yu, Q. Zeng, S. Tao, C. Xia, C. Liu, P. Liu, B. Yang, *Adv. Sci.* **2023**, *10*, 2207621; b) Y. Shi, W. Su, F. Yuan, T. Yuan, X. Song, Y. Han, S. Wei, Y. Zhang, Y. Li, X. Li, L. Fan, *Adv. Mater.* **2023**, 2210699; c) B. Wang, S. Lu, *Matter* **2022**, *5*, 110–149.
[8] M. J. Sweetman, S. M. Hickey, D. A. Brooks, J. D. Hayball, S. E. Plush, *Adv. Funct. Mater.* **2019**, *29*, 1808740.
[9] a) F. Arcudi, L. Đorđević, M. Prato, *Acc. Chem. Res.* **2019**, *52*, 2070–2079; b) X.-T. Tian, X.-B. Yin, *Small* **2019**, *15*, 1901803.
[10] S. Miao, K. Liang, J. Zhu, B. Yang, D. Zhao, B. Kong, *Nano Today* **2020**, *33*, 100879.
[11] a) S. Bhattacharyya, F. Ehrat, P. Urban, R. Teves, R. Wyrwich, M. Doblinger, J. Feldmann, A. S. Urban, J. K. Stolarczyk, *Nat. Commun.* **2017**, *8*, 1401; b) B. C. M. Martindale, G. A. M. Hutton, C. A. Caputo, S. Prantl, R.

© 2023 The Authors. Chemistry - A European Journal published by Wiley-VCH GmbH

15213765, 0, Downloaded from https://chemistry-europe.onlinelibrary.wiley.com/doi/10.1002/chem.202302850 by Universidad Autonoma De Madrid, Wiley Online Library on [08/01/2024]. See the Terms and Conditions (https://onlinelibrary.wiley.com/terms-and-conditions) on Wiley Online Library for rules of use; OA articles are governed by the applicable Creative Commons License

Godin, J. R. Durrant, E. Reisner, *Angew. Chem. Int. Ed.* **2017**, *56*, 6459–6463.
[12] H. Wang, R. Revia, K. Wang, R. J. Kant, Q. Mu, Z. Gai, K. Hong, M. Zhang, *Adv. Mater.* **2017**, *29*, 1605416.
[13] D. Qu, M. Zheng, P. Du, Y. Zhou, L. Zhang, D. Li, H. Tan, Z. Zhao, Z. Xie, Z. Sun, *Nanoscale* **2013**, *5*, 12272.
[14] L. Jiang, H. Ding, M. Xu, X. Hu, S. Li, M. Zhang, Q. Zhang, Q. Wang, S. Lu, Y. Tian, H. Bi, *Small* **2020**, *16*, 2000680.
[15] A. Stergiou, N. Tagmatarchis, *Small* **2021**, *17*, 2006005.
[16] a) F. Arcudi, V. Strauss, L. Đorđević, A. Cadranel, D. M. Guldi, M. Prato, *Angew. Chem. Int. Ed.* **2017**, *56*, 12097–12101; b) F. Arcudi, L. Đorđević, M. Prato, *Angew. Chem. Int. Ed.* **2016**, *55*, 2107–2112.
[17] M. Cacioppo, T. Scharl, L. Đorđević, A. Cadranel, F. Arcudi, D. M. Guldi, M. Prato, *Angew. Chem. Int. Ed.* **2020**, *59*, 12779–12784.
[18] a) T. Scharl, A. Ferrer-Ruiz, A. Saura-Sanmartín, L. Rodríguez-Pérez, M. A. Herranz, N. Martín, D. M. Guldi, *Chem. Commun.* **2019**, *55*, 3223–3226; b) A. Ferrer-Ruiz, T. Scharl, P. Haines, L. Rodríguez-Pérez, A. Cadranel, M. A. Herranz, D. M. Guldi, N. Martín, *Angew. Chem. Int. Ed.* **2018**, *57*, 1001–1005.
[19] L. Đorđević, P. Haines, M. Cacioppo, F. Arcudi, T. Scharl, A. Cadranel, D. M. Guldi, M. Prato, *Mater. Chem. Front.* **2020**, *4*, 3640–3648.
[20] A. Ferrer-Ruiz, T. Scharl, L. Rodríguez-Pérez, A. Cadranel, M. A. Herranz, N. Martín, D. M. Guldi, *J. Am. Chem. Soc.* **2020**, *142*, 20324–20328.
[21] J. B. Essner, G. A. Baker, *NANO* **2017**, *4*, 1216–1263.
[22] S. Collavini, F. Amato, A. Cabrera-Espinoza, F. Arcudi, L. Đorđević, I. Kosta, M. Prato, J. L. Delgado, *Energy Technol.* **2022**, *10*, 2101059.
[23] A. Privitera, M. Righetto, D Mosconi, F. Lorandi, A. A. Isse, A. Moretto, R. Bozio, C. Ferrante, L. Franco, *Phys. Chem. Chem. Phys.* **2016**, *18*, 31286–31295.
[24] S. Bettini, S. Sawalha, L. Carbone, G. Giancane, M. Prato, L. Valli, *Nanoscale* **2019**, *11*, 7414–7423.
[25] J. C. Hummelen, B. W. Knight, F. LePeq, F. Wudl, J. Yao, C. L. Wilkins, *J. Org. Chem.* **1995**, *60*, 532–538.
[26] M. M. Wienk, J. M. Kroon, W. J. H. Verhees, J. Knol, J. C. Hummelen, P. A. van Hal, R. A. J. Janssen, *Angew. Chem. Int. Ed.* **2003**, *42*, 3371–3375.
[27] V. Strauss, A. Kahnt, E. M. Zolnhofer, K. Meyer, H. Maid, C. Placht, W. Bauer, T. J. Nacken, W. Peukert, S. H. Etschel, M. Halik, D. M. Guldi, *Adv. Funct. Mater.* **2016**, *26*, 7975–7985.
[28] G. A. M. Hutton, B. C. M. Martindale, E. Reisner, *Chem. Soc. Rev.* **2017**, *46*, 6111–6123.
[29] S. L. Fronk, C.-K. Mai, M. Ford, R. P. Noland, G. C. Bazan, *Macromolecules* **2015**, *48*, 6224–6232.
[30] E. E. Maroto, A. de Cózar, S. Filippone, A. Martín-Domenech, M. Suarez, F. P. Cossío, N. Martín, *Angew. Chem. Int. Ed.* **2011**, *50*, 6060–6064.
[31] J. P. Hare, T. J. Dennis, H. W. Kroto, R. Taylor, A. W. Allaf, S. Balm, D. R. M. Walton, *J. Chem. Soc. Chem. Commun.* **1991**, 412–413.
[32] T. I. T. Okpalugo, P. Papakonstantinou, H. Murphy, J. McLaughlin, N. M. D. Brown, *Carbon* **2005**, *43*, 153–161.
[33] D. García, L. Rodríguez-Pérez, M. A. Herranz, D. Peña, E. Guitián, S. Bailey, Q. Al-Galiby, M. Noori, C. J. Lambert, D. Pérez, N. Martín, *Chem. Commun.* **2016**, *52*, 6677–6680.
[34] L. Echegoyen, L. E. Echegoyen, *Acc. Chem. Res.* **1998**, *31*, 593–601.
[35] R. Lemos, K. Makowski, L. Almagro, B. Tolón, H. Rodríguez, M. A. Herranz, D. Molero, N. Martín, M. Suárez, *Eur. J. Org. Chem.* **2023**, *26*, e202201301.
[36] G. Zatryb, M. M. Klak, *J. Phys. Condens. Matter* **2020**, *32*, 415902.
[37] A. Andreoni, L. Nardo, M. Bondani, B. Zhao, J. E. Roberts, *J. Phys. Chem. B* **2013**, *117*, 7203–7209.

Manuscript received: September 1, 2023
Accepted manuscript online: December 15, 2023
Version of record online: ■■, ■■

© 2023 The Authors. Chemistry - A European Journal published by Wiley-VCH GmbH

15213765, 0, Downloaded from https://chemistry-europe.onlinelibrary.wiley.com/doi/10.1002/chem.202302850 by Universidad Autonoma De Madrid, Wiley Online Library on [08/01/2024]. See the Terms and Conditions (https://onlinelibrary.wiley.com/terms-and-conditions) on Wiley Online Library for rules of use; OA articles are governed by the applicable Creative Commons License

RESEARCH ARTICLE

The covalent anchoring of electron acceptors derived of [6,6]-phenyl-fullerene-methyl butyrate ($PC_{61}BM$ and $PC_{71}BM$) to carbon dots (CD) was carried out successfully and the obtained hybrid nanomaterials characterized by means of AFM microscopy, and FTIR and XPS spectroscopies. Electrochemical and photophysical studies confirmed the electronic communication between the covalently connected units and their promise for further photo- and electronic applications.

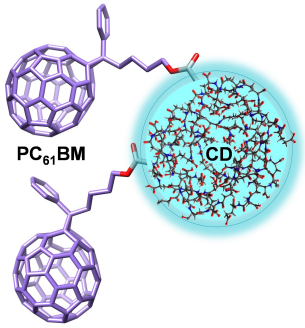

Dr. A. Ferrer-Ruiz, J. M. Moreno-Naranjo, Dr. L. Rodríguez-Pérez, Dr. S. Ramírez-Barroso, Prof. Dr. N. Martín, Prof. Dr. M. Á. Herranz**

1 – 8

n-Type Fullerene-Carbon Dots: Synthesis and Electrochemical and Photophysical Properties

15213765, 0, Downloaded from https://chemistry-europe.onlinelibrary.wiley.com/doi/10.1002/chem.202302850 by Universidad Autonoma De Madrid, Wiley Online Library on [08/01/2024]. See the Terms and Conditions (https://onlinelibrary.wiley.com/terms-and-conditions) on Wiley Online Library for rules of use; OA articles are governed by the applicable Creative Commons License